Pinedo, Carlos Eduardo; Tschiptschin, André Paulo

Low temperature plasma carburizing of AISI 316L austenitic stainless steel and AISI F51 duplex
stainless steel

Metallurgy and materials
INOX 2010

Low temperature plasma carburizing of AISI 316L austenitic stainless steel and AISI F51 duplex stainless steel

Cementação sob plasma à baixa temperatura do aço inoxidável austenítico AISI 316L e do aço inoxidável duplex AISI F51

Carlos Eduardo Pinedo

PhD, University of Mogi das Cruzes and Heat Tech Technology for Heat Treatment and Surface Engineering Ltd, Av. João XXIII 1160, ZIP 08830-000, Mogi das Cruzes, SP, Brazil. pinedo@heattech.com.br

André Paulo Tschiptschin

PhD, Professor, Metallurgical and Materials Engineering Department, University of São Paulo, Av. Prof. Mello Moraes 2463, ZIP 05508-030, São Paulo, SP, Brazil. antschip@usp.br

Abstract

In this work an austenitic AISI 316L and a duplex AISI F51 (EN 1.4462) stainless steel were DC-Plasma carburized at 480°C, using CH_4 as carbon carrier gas. For the austenitic AISI 316L stainless steel, low temperature plasma carburizing induced a strong carbon supersaturation in the austenitic lattice and the formation of carbon expanded austenite (γ_C) without any precipitation of carbides. The hardness of the carburized AISI 316L steel reached a maximum of 1000 HV due to ~13 at% carbon supersaturation and expansion of the FCC lattice. For the duplex stainless steel AISI F51, the austenitic grains transformed to carbon expanded austenite (γ_C), the ferritic grains transformed to carbon expanded ferrite (α_C) and $M_{23}C_6$ type carbides precipitated in the nitrided case. Hardness of the carburized case of the F51 duplex steel reached 1600 HV due to the combined effects of austenite and ferrite lattice expansion with a fine and dispersed precipitation of $M_{23}C_6$ carbides.

Keywords: Plasma carburizing, austenitic stainless steel, duplex stainless steel, expanded austenite, expanded ferrite.

Resumo

O aço inoxidável austenítico AISI 316L e o aço inoxidável duplex AISI F51 (EN 1.4462) foram cementados sob plasma-DC na temperatura de 480°C, utilizando-se CH_4 como gás de arraste. A cementação sob plasma à baixa temperatura conduziu a uma elevada supersaturação do reticulado cristalino em carbono com a formação de austenita expandida(γ_C), sem a precipitação de carbonetos. A dureza do aço 316L, após a cementação, atingiu um valor máximo de 1000 HV, devido à supersaturação de ~ 13 at% de carbono e à expansão do reticulado cristalino CFC. Para o aço inoxidável duplex AISI F51, os grãos de austenita se transformaram em austenita expandida pelo carbono e os grãos de ferrita se transformaram para ferrita expandida com a precipitação de carbonetos do tipo $M_{23}C_6$, na camada cementada. A dureza da camada cementada, no aço F51, atingiu 1600HV, devido ao efeito combinado da expansão dos reticulados cristalinos da austenita e da ferrita com a precipitação fina e dispersa de carbonetos $M_{23}C_6$.

Palavras-chave: *Cementação a plasma, aço inoxidável austenítico, aço inoxidável duplex, austenita expandida, ferrita expandida.*

1. Introduction

Austenitic and duplex stainless steels are widely used in a variety of applications within the chemical, refining and petrochemical industry, where high corrosion resistance and mechanical properties are required. However, the surface properties of these materials may be improved in order to reach a better performance in highly stressed tribological systems. Carbon steels have been surface hardened by nitriding diffusion processes for decades. For these steels case hardening is a consequence of nitride compound layer formation and of nitrides precipitation in the diffusion zone, namely γ'-Fe$_4$N and ε-Fe$_{2-3}$N [Cavaliere, 2009]. On the other hand, case hardening of austenitic stainless steels (ASS) by nitriding can be achieved by intensive precipitation of chromium nitrides (CrN, Cr$_2$N) in the diffusion zone during nitriding at temperatures around 500°C, increasing hardness up to 1400 HV, but decreasing the corrosion resistance [Larisch, 1999], Czerwiec, 2000], [Liang, 2000]. However, when low temperature nitriding is used, close to 400°C, the hardening mechanism changes from nitride precipitation to lattice distortion of the FCC austenitic phase, leading to formation of expanded austenite, with hardness close to 1400 HV and no loss of corrosion resistance [Fewell, 2000], Borgioli, 2005], [Mingolo, 2006]. The hardening mechanism is related to high compressive residual stresses arisen from lattice distortion.

Plasma processing of stainless steels is the most suitable case hardening process because it avoids the need of a pre-removal step of the passive Cr$_2$O$_3$ layer by chemical or mechanical operations. During plasma processing the passive layer is removed by sputtering prior to the nitriding step without any damage to the part's surface. Based on the nitrogen expanded austenite concept, low temperature carburizing has been studied for austenitic and other stainless steels types [Sun, 1999], Michal, 2006]. [Ceschini, 2008], [Souza, 2009]. In such treatments a hard and rather ductile layer increases wear properties and fatigue resistance without impairing the corrosion resistance and even increasing it in some cases. Differently from the Low Temperature Plasma Nitriding Treatment of austenitic stainless steels, where up to 35 at% of N can be introduced in austenite in solid solution, leading to the formation of a very hard (1500 HV) nitrogen rich expanded austenite (γ$_N$) layer, Low Temperature Plasma Carburizing improves the wear resistance of austenitic stainless steels through the formation of a carbon rich expanded austenite (γ$_C$) containing a maximum of 13 at% C [Cao, 2003], [Michal, 2006] in solid solution, increasing surface hardness up to 1000 HV.

Many research groups have been investigating the Low Temperature Plasma Nitriding treatment of Duplex Stainless Steels, but little is known about Low Temperature Plasma Carburizing of duplex stainless steels. [Blawert, 2000] studied low temperature plasma nitriding of a duplex (α+β) stainless steel and concluded that incorporation of nitrogen in the surface of the austenitic–ferritic steel leads to transformation of any pre-existing ferrite phase into expanded austenite. [Bielawski, 2006] studied the formation of nitrogen enriched layers, the growth of which depended on the structure and chemical composition of the matrix. They also reported a difficulty to estimate the exact character of an "expanded austenite like" layer obtained on the ferritic regions of the matrix. More recently [Bielawski, 2010] discussed the formation of expanded martensite on the ferrite grains of the matrix while [Dong, 2010] observed the coexistence of S-phase grains and N containing ferrite grains, concluding that phase identification based only on XRD is not reliable and may sometimes be misleading. [Christiansen, 2009] reported that a SAF 2507 superduplex stainless steel showed a different nitriding response with the formation of a thick layer of expanded austenite, in both ferrite and austenite grains of the matrix. On the other hand the same authors observed that nitriding an AISI 329 at 450°C produced a thick nitride layer with marked differences between austenite and ferrite: the nitriding temperature was too high with regard to development of γ$_N$ in ferrite, leading to precipitation of very fine nitrides in ferrite, while no precipitates could be seen in the expanded austenite phase. This behavior was attributed to the higher content of chromium in the ferritic phase [Christiansen, 2005]. [Michal, 2009], on the other hand, found that after low temperature plasma carburizing an AISI 301 stainless steel, containing approximately 40% of ferrite, the ferrite peaks disappeared and the austenite peaks have shifted to smaller 2θ angles, indicating an expansion of ~3 % on the lattice parameter of austenite.

The aim of this work is to present results of low temperature plasma carburizing of an AISI 316L austenitic and an AISI F51 duplex stainless steel. Changes in the surface microstructure, as well as its influence on hardening are presented.

2. Materials and methods

Annealed round bars of commercial austenitic AISI 316L (ASS) and duplex AISI F51 (DSS) stainless steels were sliced into 3 mm thick specimens, mechanically ground and polished with diamond paste down to 1μm, prior to plasma carburizing. The chemical compositions of both steels are shown in Table 1.

Low temperature plasma carburizing (LTPC) was carried out in a pulsed plasma reactor with a hot wall chamber. Passive film was removed by a sputtering step conducted at 400°C for 1 hour using high intensity pure hydrogen plasma. Carburizing was conducted at 480°C, during 12 hours. A gas mixture composition of 18(l/h)H$_2$:6(l/h)Ar:180(cl/h)CH$_4$ was used. During the treatment the carburizing temperature was measured by two thermocouples embedded in the samples.

The phases formed in the carburized layer were identified by XRD in a Phillips diffractometer using CuK$_α$ radiation, λ

	C	Si	Mn	Cr	Ni	Mo	N
AISI 316L	0.015	0.33	1.82	17.37	14.51	2.82	0.075
AISI F51	0.030	0.69	1.02	21.16	6.55	2.76	0.147

Table 1
Chemical composition (wt %).

= 0.1542 nm, with a conventional θ/2θ Bragg-Brentano symmetric geometry. The

surface hardness of the carburized samples was measured using a Shimadzu Vickers

microhardness system with a 50 g load.

3. Results and discussion

LTPC AISI 316L Austenitic Stainless Steel

X-ray diffraction patterns of the AISI 316L austenitic stainless steel before and after plasma carburizing are shown in Figure 1. Compared to the untreated austenite, the diffraction peaks are broader and shifted to lower diffraction angles, characteristics of carbon expanded austenite (γ_C) similar to the nitrogen expanded austenite (γ_N) identified by other authors after plasma nitriding a 316L austenitic stainless steel [Liang, 2000]. Very high compressive stresses develop in the FCC lattice due to carbon supersaturation

increasing the austenite lattice parameter up to 0.369 nm. For comparison, the FCC lattice parameter of the untreated austenite was evaluated as a = 0.359 nm, and that available from JCPDS-ICDD® data files is a = 0.360 nm [ICDD, 1955]. The relative expansion of austenite lattice parameter (γ_C) when compared to the untreated austenite (Δa/a) was calculated as 2.8%. According to [Christiansen, 2009] the lattice parameter of 0.369 nm corresponds to carbon occupancy Yc in the lattice of 15% or around 3 wt% C in

solid solution in austenite.

Figure 2 shows that the surface hardness after plasma carburizing AISI 316L ASS increased up to 1010 HV0.05. Compared to the hardness of the solution treated state, 181 HV0.05, the plasma carburizing treatment increases the hardness more than five times. Considering that Austenitic Stainless Steels are not prone to be hardened by heat treatment, this surface treatment should potentially be used to increase tribological properties and service performance.

Figure 1
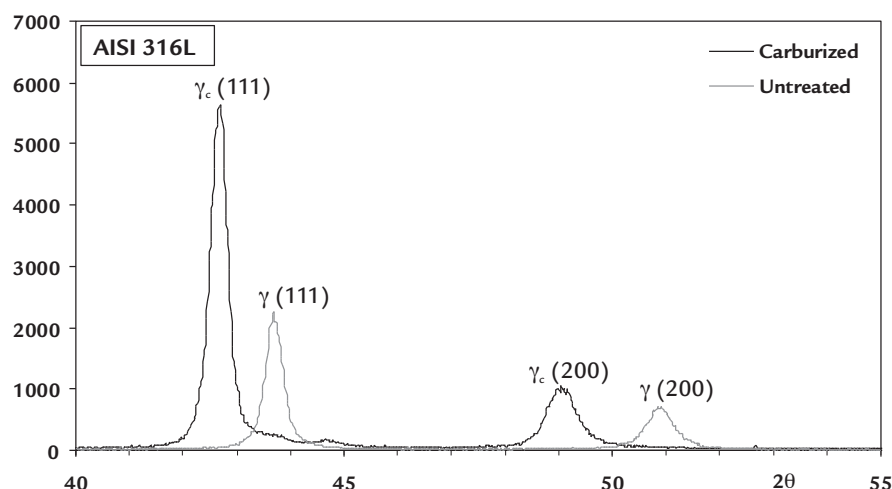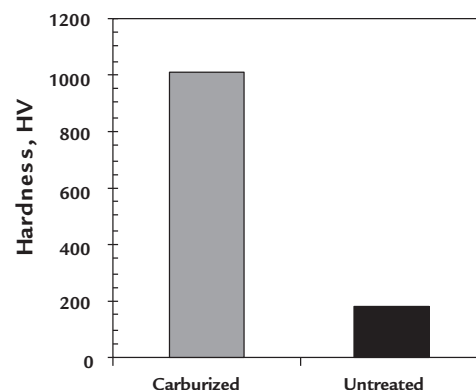XRD diffraction patterns for AISI 316L steel before and after carburization.

Figure 2
Surface hardness after low temperature plasma carburizing AISI 316L ASS.

LTPC AISI F51 Duplex Stainless Steel

Figure 3 shows X-ray diffraction patterns for the solubilized and LTPC AISI F51 DSS. Before carburizing peaks referring to ferrite and austenite can be observed. The calculated lattice parameters for ferrite and austenite are 0.287 nm and 0.359 nm, respectively, close to those informed on ICDD files [ICDD, 1955], [ICDD, 1949] 0.286 nm and 0.360 nm.

After carburizing the high intensity ferrite (110) and austenite (111) diffraction peaks got broader and shifted to lower diffraction angles, indicating lattice expansion of both phases. The high intensity broad peak 2θ = 44.3° is the result of three different contributions: a) α_C (110) carbon expanded ferrite; b) γ_C (111) expanded austenite and c) $M_{23}C_6$ (511) carbide

[ICDD, 1949] #78-1500 - $Cr_{21.34}Fe_{1.66}C_6$ [ICDD, 1949]. A second carbon expanded ferrite peak, α_C (200) can be seen for 2θ = 64.1°. Less defined peaks could be also identified for 2θ = 43.3° and 2θ = 49.2° corresponding to expanded austenite γ_C (111) and γ_C (200), respectively.

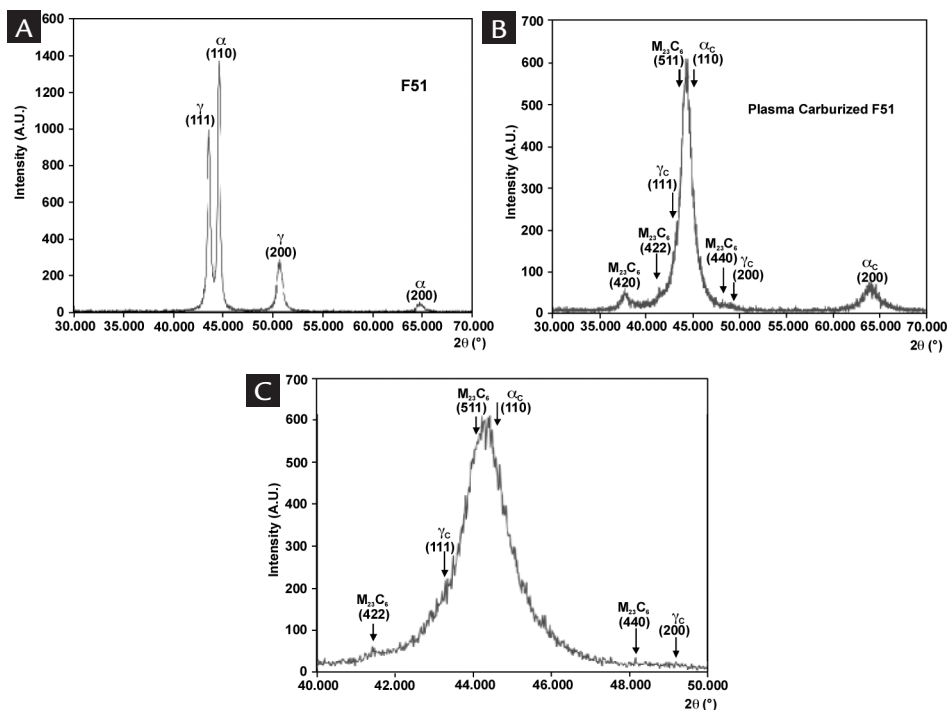Christiansen et al. reported intense precipitation of cubic chromium nitrides

Figure 3
(A) XRD diffraction patterns for AISI F51 steel (a) before and (b) after carburization and (c) detail of the superimposed α_C (110) carbon expanded ferrite, γ_C (111) expanded austenite and $M_{23}C_6$ (511) carbides peaks.
(B) XRD diffraction patterns for AISI F51 steel (a) before and (b) after carburization and (c) detail of the superimposed α_C (110) carbon expanded ferrite, γ_C (111) expanded austenite and $M_{23}C_6$ (511) carbides peaks.
(C) XRD diffraction patterns for AISI F51 steel (a) before and (b) after carburization and (c) detail of the superimposed α_C (110) carbon expanded ferrite, γ_C (111) expanded austenite and $M_{23}C_6$ (511) carbides peaks.

CrN in ferrite during plasma nitriding of an AISI 329 duplex stainless steel at 450°C [Christiansen, 2005]. The ferritic phase of the plasma carburized layer appeared darkly etched as a consequence of intense precipitation of finely dispersed chromium nitrides. Figure 4 shows the carburized layer of the F51 duplex stainless steel, where it can be seen intense precipitation of $M_{23}C_6$ carbides inside ferritic grains in the layer, as well.

Low temperature plasma carburizing of AISI F51 DSS led, also, to strong surface hardening, as a consequence of the contribution of residual stresses associated to the carbon induced expansion of both FCC and BCC lattices and to very fine precipitation of $M_{23}C_6$ carbides, known to induce secondary hardening at temperatures near 500°C. In this case the hardening effect is much higher than that observed for the 316L ASS due to very fine and dispersed precipitation of carbides in ferrite and austenite in the carburized layer. Figure 5 shows the carburized surface of the specimen, on top of which HV 0.05 microhardness were taken. Both phases, ferrite and austenite, were strongly hardened due to carbon supersaturation and fine carbide precipitation, reaching hardness up to 1600 HV 0.05.
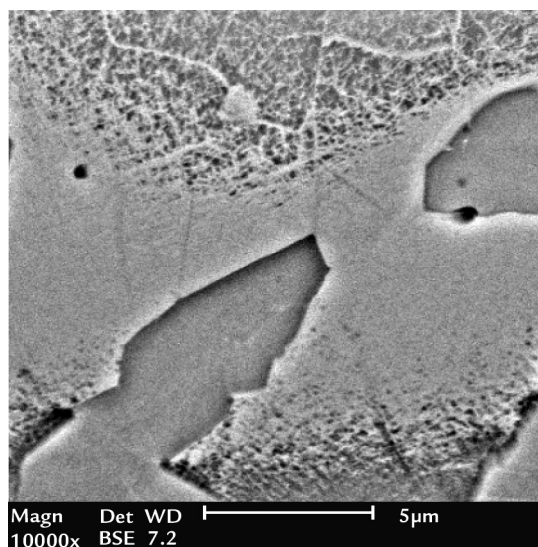

Figure 4
Micrograph of the carburized layer. Precipitated $M_{23}C_6$ carbides are seen in ferritic and austenitic grains in the layer.

4. Conclusions

Carbon expanded austenite was obtained after low temperature plasma carburizing (LTPC) of AISI 316L Austenitic Stainless Steel. High compressive stresses were induced in the carburized case by carbon supersaturation and a surface hardness of 1000 HV0.05 was achieved.

For the Duplex Stainless Steel AISI F51, the starting austenitic-ferritic microstructure got supersaturated in carbon leading to the formation of carbon expanded austenite (γ_C), carbon expanded ferrite (α_C) and precipitation of $M_{23}C_6$ carbides. As a consequence of austenite and ferrite lattice expansions, associated to fine $M_{23}C_6$ carbide precipitation, a strong hardening effect, up to 1600 HV0.05, was observed.

Figure 5
(A) Surface hardness after low temperature plasma carburizing AISI F51 DSS and (B) SEM image showing measurements of Vickers indentations.
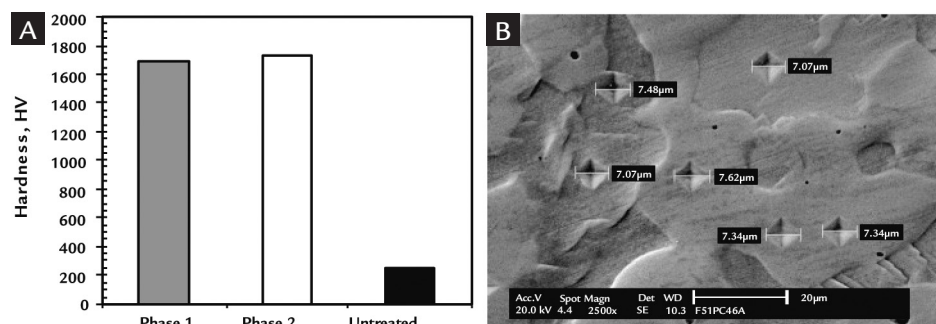
5. Acknowledgements

6. References

BIELAWSKI, J., BARANOWSKA, J., SZCZECINSKI, K. Microstructure and properties of layers on chromium steel. *Surface and Coatings Technology*, 200, p. 6572-6577, 2006.

BIELAWSKI, J., BARANOWSKA, J. Formation of nitrided layers on duplex steel - influence of multiphase substrate. *Surface Engineering*, n. 26, p. 299-304, 2010.

BLAWERT, C., MORDIKE, B.L., JIRÁSKOVA, Y., SCHNEEWEISS, O. Structure and composition of expanded austenite produced by nitrogen plasma immersion ion implantation of stainless steels X6CrNiTi1810 and X2CrNiMoN2253. *Surface and Coatings Technology*, 116-119, p.189-198, 2000.

BORGIOLI, F., FOSSATI, A., GALVANETTO, E., BACCI, T. Glow-discharge nitriding of AISI 316L austenitic stainless steel: influence of treatment temperature. *Surface and Coatings Technology*, 200, p. 2474-2480, 2005.

CAO Y., ERNST F., HEUER A.H. Colossal carbon supersaturation in austenitic stainless steels carburized at low temperature. *Acta Materialia*, 5n. 1, p. 4171-4181, 2003.

CAVALIERE, P., ZAVARISE, G., PERILLO, M. Modeling carburizing and nitriding processes. *Computational Materials Science*, n. 46, p. 26-35, 2009.

CESCHINI, L. MINAK, G. Fatigue behaviour of low temperature carburized AISI 316L austenitic stainless steel, *Surface and Coatings Technology*, 202, p. 1778-1784, 2008.

CHRISTIANSEN, T.L., SOMERS, M.A.J. Low temperature gaseous nitriding and carburizing of stainless steels. *Surface Engineering*, n. 21, p. 445-455, 2005.

CHRISTIANSEN, T.L., SOMERS, M.A.J. Low temperature gaseous surface hardening of stainless steel: the current status. *International Journal Materials Research*, 100, p. 1361-1377, 2009.

CZERWIEC, T., RENEVIER, N., MICHEL, H. Low-temperature plasma-assisted nitriding. *Surface and Coatings Technology*, 131, p. 267-277, 2000.

DONG, H. S-phase surface engineering of Fe-Cr, Co-Cr and Ni-Cr alloys. *International Materials Reviews*, n. 55, p. 65-98, 2010.

FEWELL, M.P., MICHEL, D.R.G., PRIEST, J.M., SHORT, K.T., COLLINS, G.A. The nature of expanded austenite. *Surface and Coatings Technology*, 131, p. 300-306, 2000.

ICDD INTERNATIONAL CENTRE FOR DIFFRACTION DATA, H.E. Swanson et al., Nat. Bur. Stand (U.S.), Circ. 509, 4, 3 (1955).

ICDD INTERNATIONAL CENTRE FOR DIFFRACTION DATA, H.J. Goldschmidt. *Metallurgia*, v. 40, n. 103, 1949.

LARISCH, B., BRUSKY, U., SPIES, H-J. Plasma nitriding stainless steels at low temperature. *Surface and Coatings Technology*, 116-119, 205-211, 1999.

LIANG, W., BIN, X., ZHIWEI, Y., YAQIN, S. The wear and corrosion properties of stainless steel nitrided by low-pressure plasma-arc source ion nitriding at low temperatures. *Surface and Coatings Technology*, 130, p. 304-308, 2000.

MICHAL, G.M., ERNST, F., KAHN, H., CAO, Y., AGARWAL, N., HEUER, A.H. Carbon supersaturation due to paraequilibrium carburization: Stainless steels with greatly improved mechanical properties. *Acta Materialia*, n. 54, p. 1597-1606, 2006.

MICHAL, G.M., GU, X., JENNINGS, W.D., KAHN, H., ERNST, F., HEUER, A.H., Paraequilibrium Carburization of Duplex and Ferritic Stainless Steels. *Metallurgical and Materials Transactions A*, 40A, p. 1781-1790, 2009.

MINGOLO, N., PINEDO, C.E., TSCHIPTSCHIN, A.P. On the formation of expanded austenite during plasma nitriding of an AISI 316L austenitic stainless steel, *Surface and Coatings Technology*, 201, p. 4215-4218, 2006.

SUN, Y., LI, X., BELL, T. Low temperature plasma carburizing of austenitic stainless steels for improved wear and corrosion resistance. *Surface Engineering*, n. 15, p. 49-54, 1999.

SOUZA, R.M., IGNAT, M., PINEDO C.E., TSCHIPTSCHIN, A.P. Structure and properties of low temperature plasma carburized austenitic stainless steel. *Surface and Coatings Technology*, 204, p. 1102-1105, 2009.